

ARMY RESEARCH LABORATORY



Design and Analysis of a 15-kV Package for Wide Bandgap Semiconductor Devices

by Dimeji Ibitayo and C. Wesley Tipton

ARL-TR-3225

May 2004

NOTICES

Disclaimers

The findings in this report are not to be construed as an official Department of the Army position unless so designated by other authorized documents.

Citation of manufacturer's or trade names does not constitute an official endorsement or approval of the use thereof.

Destroy this report when it is no longer needed. Do not return it to the originator.

Army Research Laboratory

Adelphi, MD 20783-1197

ARL-TR-3225

May 2004

**Design and Analysis of a 15-kV Package for Wide Bandgap
Semiconductor Devices**

**Dimeji Ibitayo and C. Wesley Tipton
Sensors and Electron Devices Directorate, ARL**

REPORT DOCUMENTATION PAGE			Form Approved OMB No. 0704-0188		
Public reporting burden for this collection of information is estimated to average 1 hour per response, including the time for reviewing instructions, searching existing data sources, gathering and maintaining the data needed, and completing and reviewing the collection information. Send comments regarding this burden estimate or any other aspect of this collection of information, including suggestions for reducing the burden, to Department of Defense, Washington Headquarters Services, Directorate for Information Operations and Reports (0704-0188), 1215 Jefferson Davis Highway, Suite 1204, Arlington, VA 22202-4302. Respondents should be aware that notwithstanding any other provision of law, no person shall be subject to any penalty for failing to comply with a collection of information if it does not display a currently valid OMB control number. PLEASE DO NOT RETURN YOUR FORM TO THE ABOVE ADDRESS.					
1. REPORT DATE (DD-MM-YYYY) May 2004		2. REPORT TYPE Final		3. DATES COVERED (From - To)	
4. TITLE AND SUBTITLE Design and Analysis of a 15-kV Package for Wide Bandgap Semiconductor Devices			5a. CONTRACT NUMBER		
			5b. GRANT NUMBER		
			5c. PROGRAM ELEMENT NUMBER		
6. AUTHOR(S) Dimeji Ibitayo and C. Wesley Tipton			5d. PROJECT NUMBER		
			5e. TASK NUMBER		
			5f. WORK UNIT NUMBER		
7. PERFORMING ORGANIZATION NAME(S) AND ADDRESS(ES) U.S. Army Research Laboratory ATTN: AMSRD-ARL-SE-DP 2800 Powder Mill Road Adelphi, MD 20783-1197			8. PERFORMING ORGANIZATION REPORT NUMBER ARL-TR-3225		
9. SPONSORING/MONITORING AGENCY NAME(S) AND ADDRESS(ES) U.S. Army Research Laboratory 2800 Powder Mill Road Adelphi, MD 20783-1197			10. SPONSOR/MONITOR'S ACRONYM(S)		
			11. SPONSOR/MONITOR'S REPORT NUMBER(S)		
12. DISTRIBUTION/AVAILABILITY STATEMENT Approved for public release; distribution unlimited.					
13. SUPPLEMENTARY NOTES					
14. ABSTRACT The development of wide bandgap semiconductor materials such as silicon carbide (SiC) has made possible devices that exceed the voltage ratings of conventional component packaging schemes. As such, a new class of high voltage packages must be developed to realize the full potential of these technologies. We report on the electrostatic analysis and design of a 15-kV ceramic package using the ANSYS ¹ Multiphysics software. To baseline our work, a standard ceramic package was characterized and modeled for high voltage operation. With this information, a new package geometry was designed, and additional SiC die requirements were identified via finite element simulations. ¹ Not an acronym.					
15. SUBJECT TERMS 15 kV package, SiC, ANSYS					
16. SECURITY CLASSIFICATION OF:			17. LIMITATION OF ABSTRACT UL	18. NUMBER OF PAGES 18	19a. NAME OF RESPONSIBLE PERSON Dimeji Ibitayo
a. REPORT Unclassified	b. ABSTRACT Unclassified	c. THIS PAGE Unclassified			19b. TELEPHONE NUMBER (Include area code) 301-394-5514

Contents

List of Figures	iv
List of Tables	iv
1. Introduction	1
2. Modeling/Design	1
3. Experimentation	8
4. Summary	10
Distribution List	11

List of Figures

Figure 1. Standard package geometry.....	2
Figure 2. Electric field plot at the lead region of the standard package.....	2
Figure 3. High-voltage package geometry.....	3
Figure 4. Electric field plot at the lead region of the high-voltage package.....	3
Figure 5. Electric field plots showing the performance of Fluorinert under an applied voltage of 15 kV with surface potential terminated 0.2 mm from the edge of the die.....	4
Figure 6. Electric field plot showing the performance of Fluorinert under an applied voltage of 15 kV with surface potential terminated 0.5 mm from the edge of the die.....	4
Figure 7. Electric field plot showing the performance of the epoxy under an applied voltage of 15 kV with surface potential terminated 0.2 mm away from the edge of the die.....	5
Figure 8. Electric field plot showing the performance of the epoxy under an applied voltage of 15 kV with surface potential terminated 0.5 mm away from the edge of the die.....	5
Figure 9. Electric field plot showing the performance of Fluorinert under an applied voltage of 10 kV with surface potential terminated 0.2 mm from the edge of the die.....	6
Figure 10. Electric field plot showing the performance of SF ₆ under an applied voltage of 10 kV with surface potential terminated 0.2 mm away from the edge of the die.....	7
Figure 11. Electric field plot showing the performance of SF ₆ under an applied voltage of 10 kV with surface potential terminated 0.5 mm away from the edge of the die.....	7
Figure 12. Electric field plot of Vendor A package showing failure at 1.8 kV.....	8
Figure 13. Photograph of Vendor B package showing where arcing occurred.....	9
Figure 14. Electric field plot of the Vendor B package under 8-kV operation.....	9

List of Tables

Table 1. Material properties.....	1
-----------------------------------	---

1. Introduction

This analysis was performed in support of the Defense Advanced Research Projects Agency Wide Band-gap Initiative High Power Electronics program. One of the goals of this program is to demonstrate silicon carbide (SiC) technology for use in high voltage applications. The U.S. Army Research Laboratory performed a series of electrostatic analyses to determine the appropriate package geometry for 10- to 15-kV devices. In these analyses, the operating ambient was assumed to be at 25 °C. These finite element analyses were coupled with high voltage experimentation for validation purposes.

2. Modeling/Design

The primary tool used in these analyses was ANSYS¹. ANSYS is a finite element analysis modeling software package used in a variety of engineering applications. An electrostatic field analysis was performed to determine the electric field distribution caused by applied voltage. The procedure for doing the electrostatic analysis consisted of three main phases using a combination of the ANSYS graphical user interface (GUI) and commands: (1) build the model, (2) apply loads and obtain solution, and (3) review results.

To build the model, the preferences were set for an electric analysis: This was done to ensure that the elements needed for the analysis were available. Once the electric preference was set, the ANSYS preprocessor (PREP7) was used to define the element type, the material properties, and the model geometry. These tasks are common to most analyses. The element type used was PLANE121, the ANSYS 2-D, eight-node electrostatic element. For an electrostatic analysis, the permittivity (PERX) material property must be defined. Table 1 provides the permittivities of the materials used in the simulations as well as their corresponding breakdown, electric field strengths.

Table 1. Material properties.

Material	Relative permittivity	Field strength (MV/m)
Air	1.0001	3
Alumina	9.5	16.9
*Epoxy	4.0	22
Fluorinert	1.98	15.75
SiC	10.2	300
SF ₆ [†]	1.0021	9

*Duralco 4460

†Sulfur hexafluoride

¹Not an acronym.

Figure 1 shows a comparison of a “standard” design as modeled in ANSYS. The light blue areas represent the ambient environments that were varied among several materials including air, epoxy, Fluorinert, and SF₆. These materials were evaluated as encapsulants. The white areas are alumina, the orange areas are metals (lead, bond wires, and base plate), and the black area is the silicon carbide die. The silicon carbide die had a metallized top surface, the extent of which was varied. After the areas were created, they were meshed.

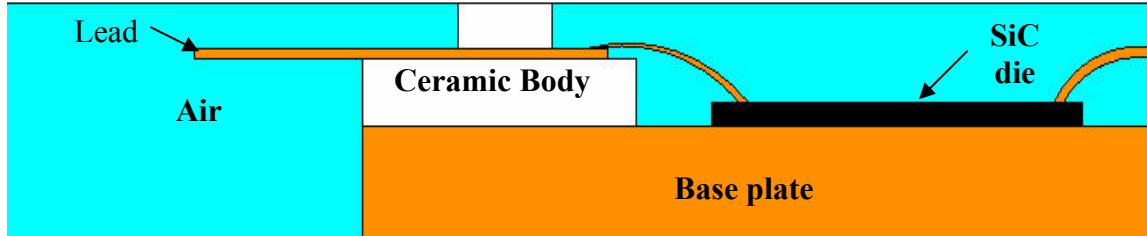


Figure 1. Standard package geometry.

When the meshing procedure was complete, the second step of the analysis was to apply loads and solve. Voltage loads were applied in these analyses. Voltage loads of 10 to 15 kV were applied to the metal lead, the wire bonds, and the metallized top surface of the die. The base plate was at zero potential with an applied voltage of 0 V. After the loads were applied, the solution was obtained.

The final step of the analysis was to review results. The ANSYS finite element analysis program generated electric field plots of the various geometrical and material configurations. Figure 2 shows the simulations results for the package shown in figure 1. In the simulations, package failure occurs if the critical field of the dielectric (air) is exceeded so that a high-field path exists between two conductors. Figure 2 shows that a high electric field (>3 MV/m for air) exists between the package lead and base plate.

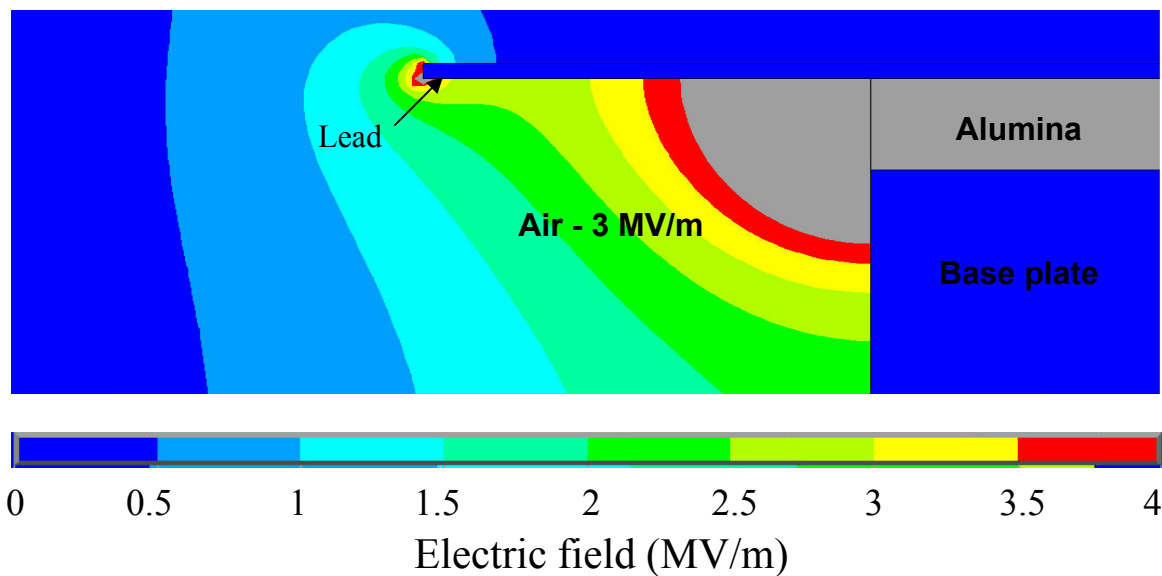


Figure 2. Electric field plot at the lead region of the standard package.

In order to eliminate the continuous breakdown region, a new package was designed with the ceramic body extended beyond the base plate. Figures 3 and 4 show the geometry of the new high-voltage package design and the electric field plot, respectively. The extended body simulation of figure 4 shows that the continuous breakdown region has been eliminated.

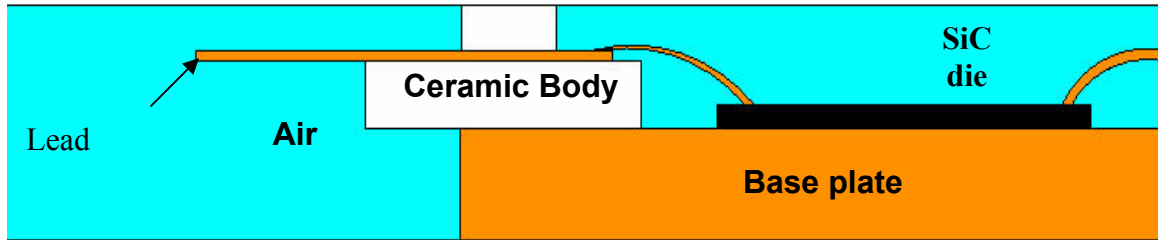


Figure 3. High-voltage package geometry.

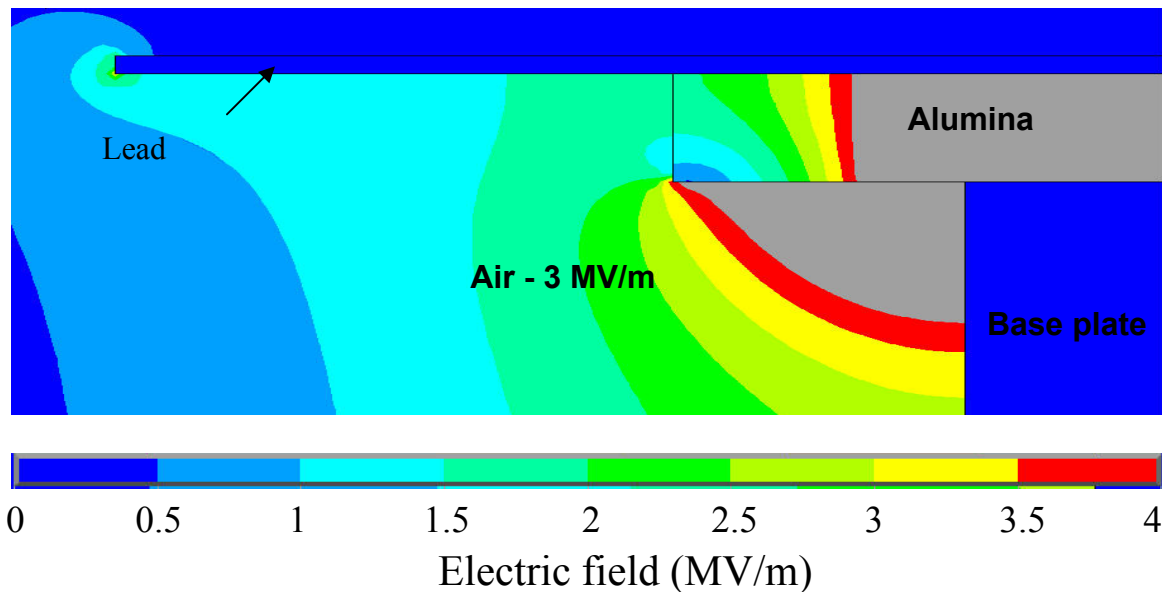


Figure 4. Electric field plot at the lead region of the high-voltage package.

Although it was possible to design the lead region of the package for high-voltage operation in air, the same was not the case for inside the package cavity. Extensive finite element analysis was conducted, but it was discovered that the high-voltage package required encapsulants with significantly higher dielectric strengths than air to successfully operate at voltages of 10 to 15 kV. The extent of potential termination from the edge of the die was also a crucial factor. Simulations were conducted with 0.2- and 0.5-mm termination spacing. Figure 5 shows the electric field near the silicon carbide die at an operating voltage of 15 kV. In this simulation, Fluorinert was used as an encapsulant and the potential was terminated 0.2 mm from the edge of the die. Figure 6 shows the electric field distribution under the same conditions as figure 5 except that the potential is terminated 0.5 mm from the die edge. With Fluorinert's electric field strength of approximately 15 MV/m, the simulation indicates that the potential on the die should be terminated greater than 0.2 mm from the edge to prevent breakdown at 15 kV.

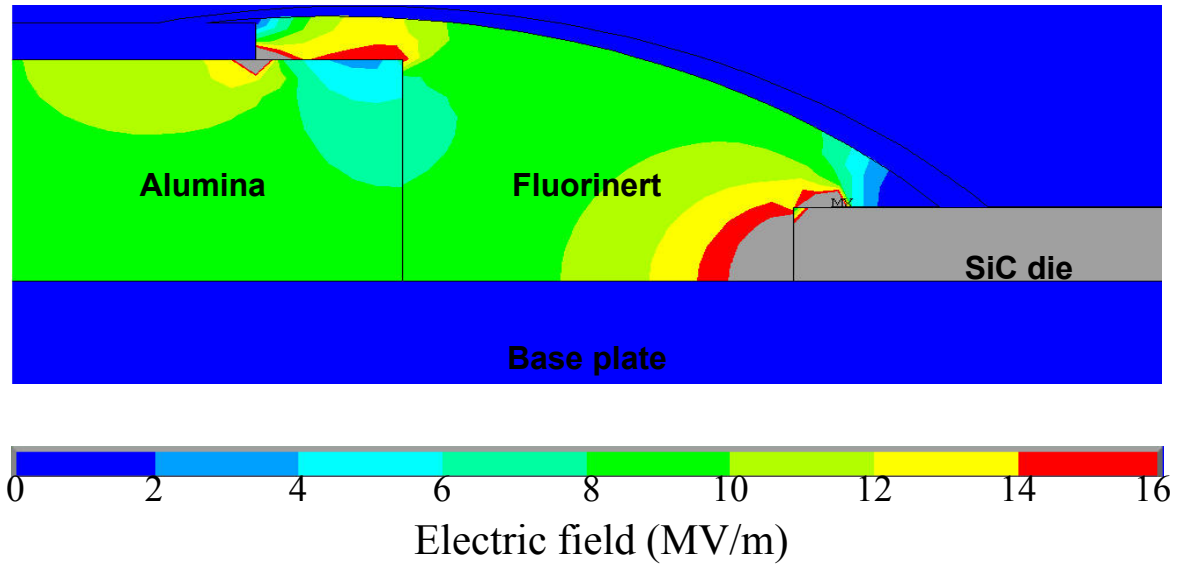


Figure 5. Electric field plots showing the performance of Fluorinert under an applied voltage of 15 kV with surface potential terminated 0.2 mm from the edge of the die.

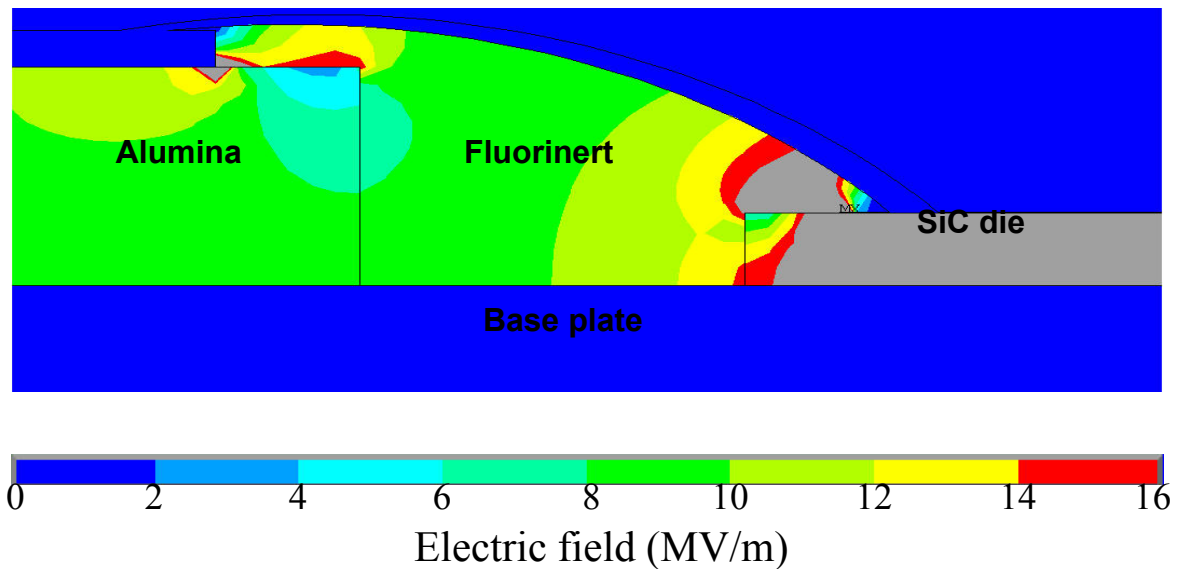


Figure 6. Electric field plot showing the performance of Fluorinert under an applied voltage of 15 kV with surface potential terminated 0.5 mm from the edge of the die.

Figure 7 shows the electric field near the silicon carbide at an applied voltage of 15 kV and with the epoxy encapsulant. The potential was terminated 0.2 mm from the edge of the die. Figure 8 shows the electric field distribution under the same conditions as figure 7 except that the potential was terminated 0.5 mm from the die edge. With an electric field strength of approximately 22 MV/m, the result indicates that the epoxy provides for a reasonable dielectric breakdown margin at a termination spacing of 0.2 mm.

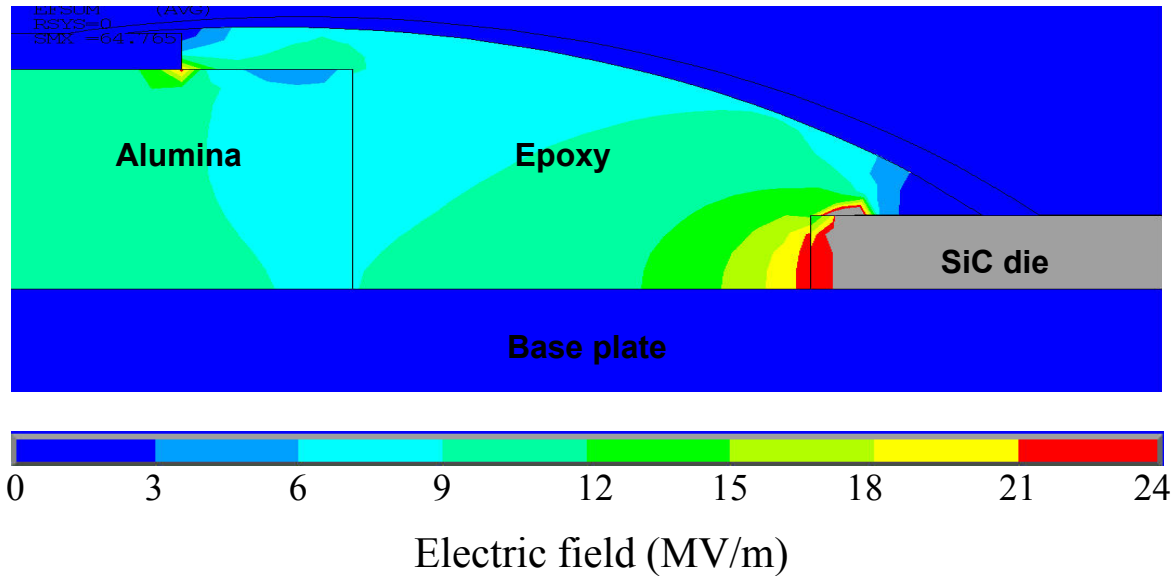


Figure 7. Electric field plot showing the performance of the epoxy under an applied voltage of 15 kV with surface potential terminated 0.2 mm away from the edge of the die.

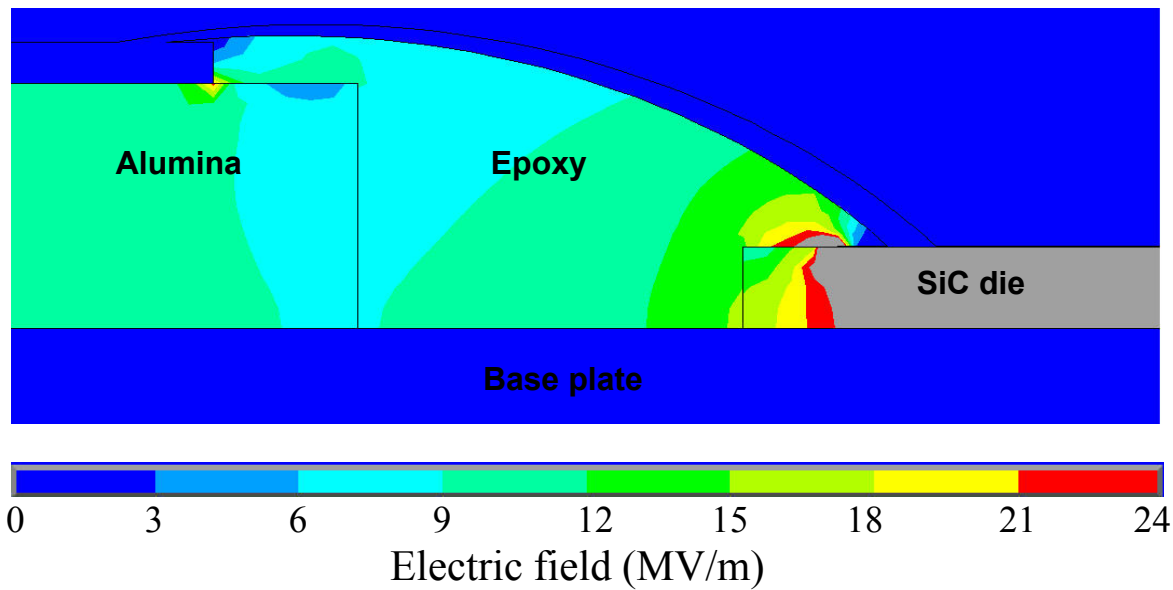


Figure 8. Electric field plot showing the performance of the epoxy under an applied voltage of 15 kV with surface potential terminated 0.5 mm away from the edge of the die.

Figures 5 through 8 show that when the surface is terminated approximately 0.2 mm from the edge of the die at 15 kV, the epoxy alone can be successfully used as the encapsulant. Fluorinert will also be effective at this voltage if the termination is 0.5 mm or farther from the edge of the die. However, it was discovered from further analyses that materials that have considerably lower dielectric strengths than Fluorinert (e.g., SF₆ at 9 MV/m) cannot be considered as encapsulants for this package at 15 kV.

The package was also simulated at 10 kV. Figure 9 shows the electric field near the silicon carbide die at an applied voltage of 10 kV. In this simulation, Fluorinert was used as an encapsulant and the potential was terminated 0.2 mm from the edge of the die. With Fluorinert's electric field strength of approximately 15 MV/m, it provides for a reasonable dielectric breakdown margin at a termination spacing of 0.2 mm.

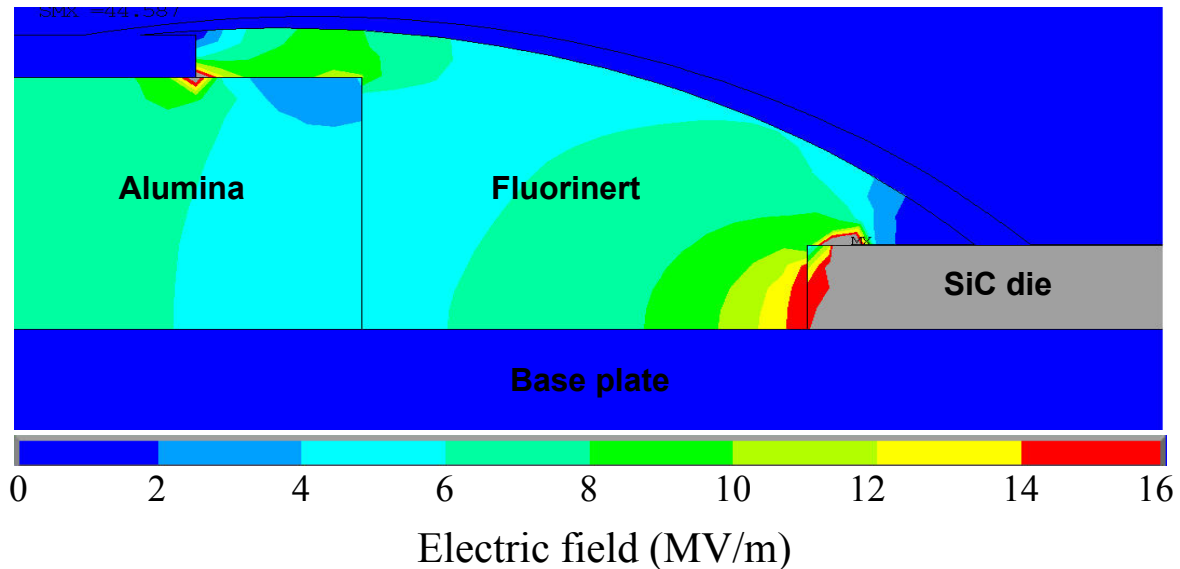


Figure 9. Electric field plot showing the performance of Fluorinert under an applied voltage of 10 kV with surface potential terminated 0.2 mm from the edge of the die.

The performance of SF₆ was also investigated at 10 kV. SF₆ is one of the most popular insulating gases with a breakdown strength of about 3 times that of air. It is important to note that this gas is fairly inert at normal temperatures, but it presents hazards at elevated temperatures because it can decompose to form fluorine, which is highly reactive. Figure 10 shows that at a termination spacing of 0.2 mm, SF₆ is not able to protect against breakdown at 10 kV. However, as seen in figure 11, it does provide a reasonable breakdown margin with a 0.5-mm termination spacing.

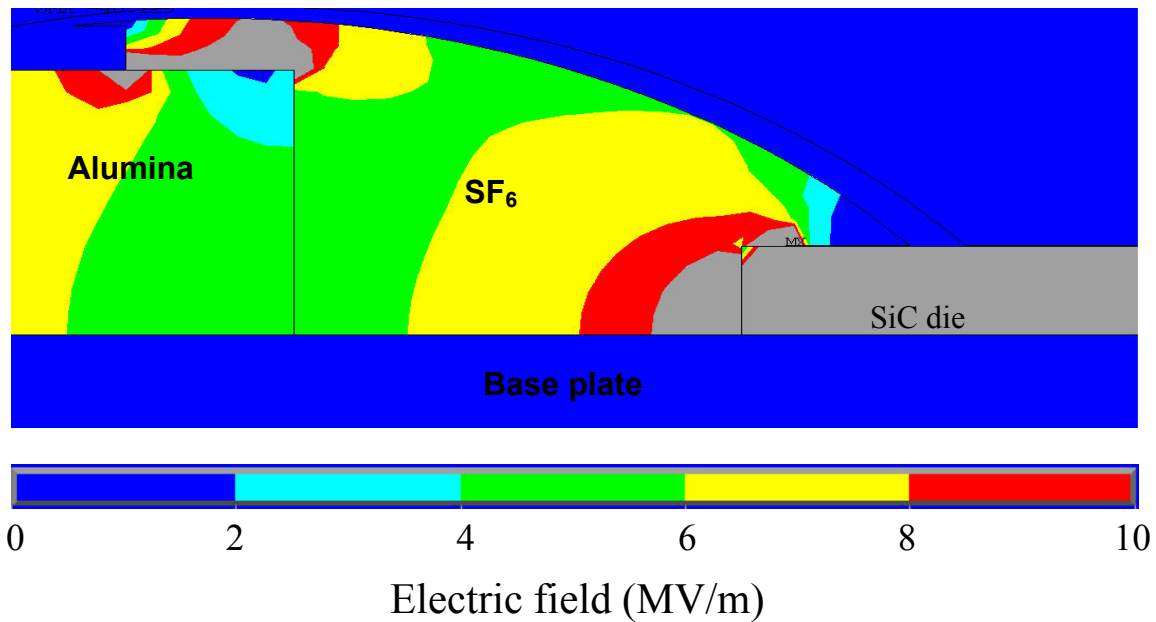


Figure 10. Electric field plot showing the performance of SF₆ under an applied voltage of 10 kV with surface potential terminated 0.2 mm away from the edge of the die.

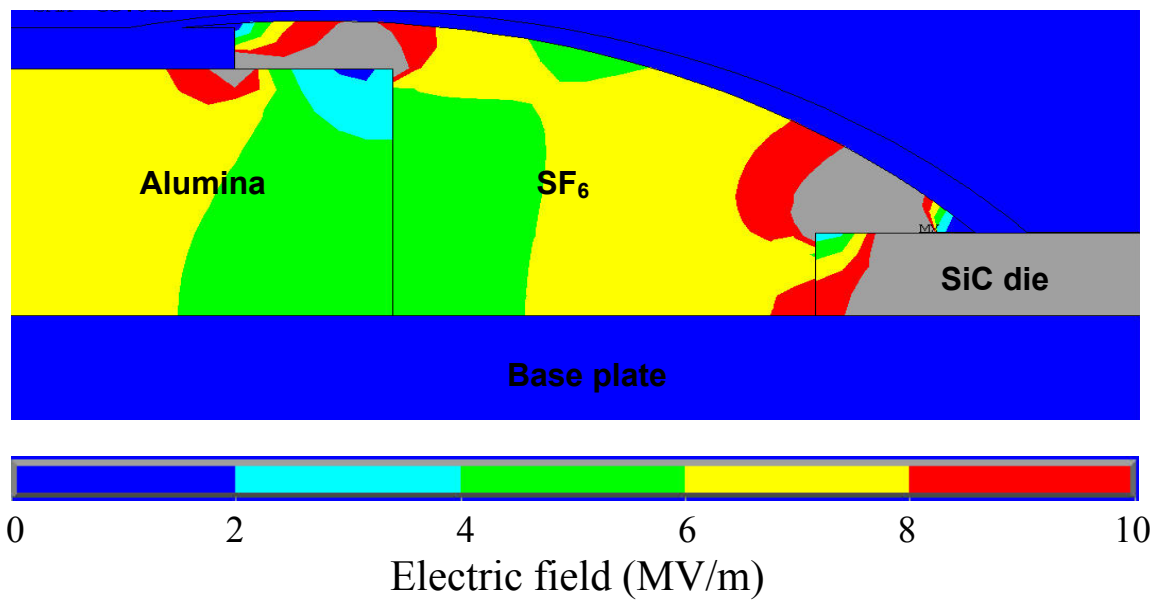


Figure 11. Electric field plot showing the performance of SF₆ under an applied voltage of 10 kV with surface potential terminated 0.5 mm away from the edge of the die.

3. Experimentation

In order to validate the electrostatic finite element analysis, several standard ceramic packages were characterized for high voltage operation. The first ceramic package from Vendor A was rated at 2 kV. When the package was characterized under a curve tracer in the operating ambient, it failed at 1.5 kV. For this same package, ANSYS results indicate that breakdown will occur at approximately 1.8 kV. Figure 12 shows the ANSYS simulation for this particular package at 1.8 kV. The lead and cavity regions are shown on the same plot.

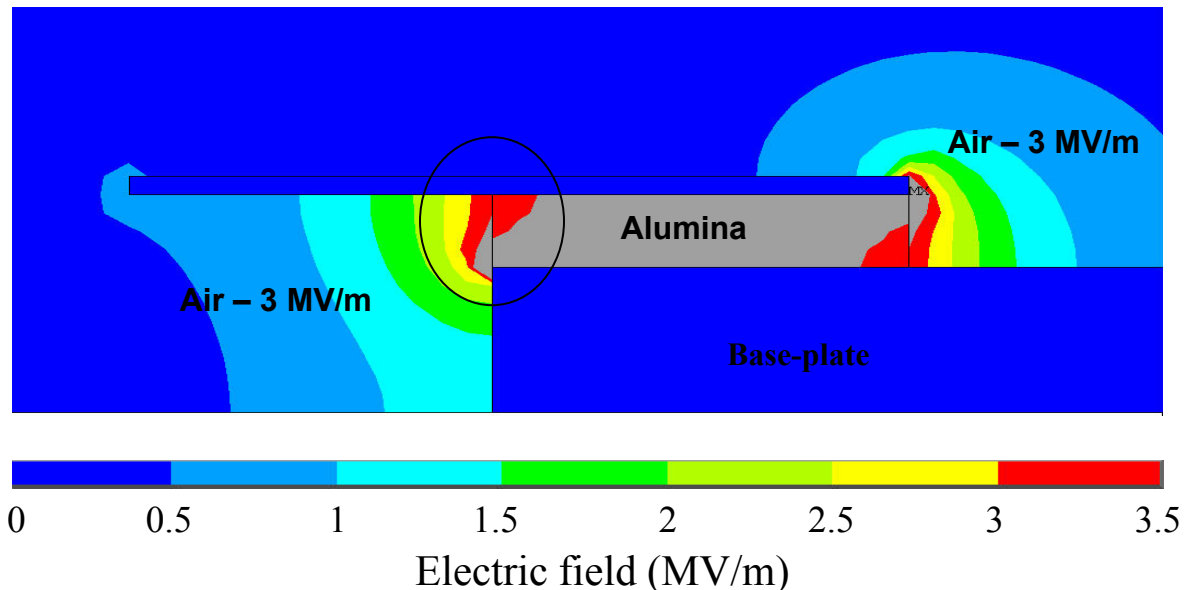


Figure 12. Electric field plot of Vendor A package showing failure at 1.8 kV.

A ceramic package from Vendor B was also characterized for high voltage operation. This package is a slightly different design from the Vendor B package, and the ceramic body is 5 times thicker. The characterization of this package was conducted with a 10-kV power supply in a nitrogen atmosphere. The package failed at 7.8 kV because of arcing between the metal lead and the metallized backside surface of the ceramic ring as shown in figure 13.

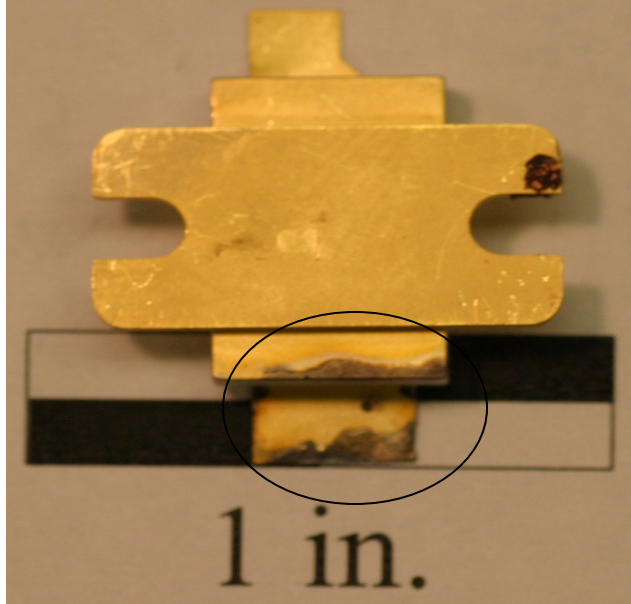


Figure 13. Photograph of Vendor B package showing where arcing occurred.

ANSYS results show that dielectric breakdown will take place at around 8 kV, based on figure 14. Analysis error for this package is calculated to be 2.56 %.

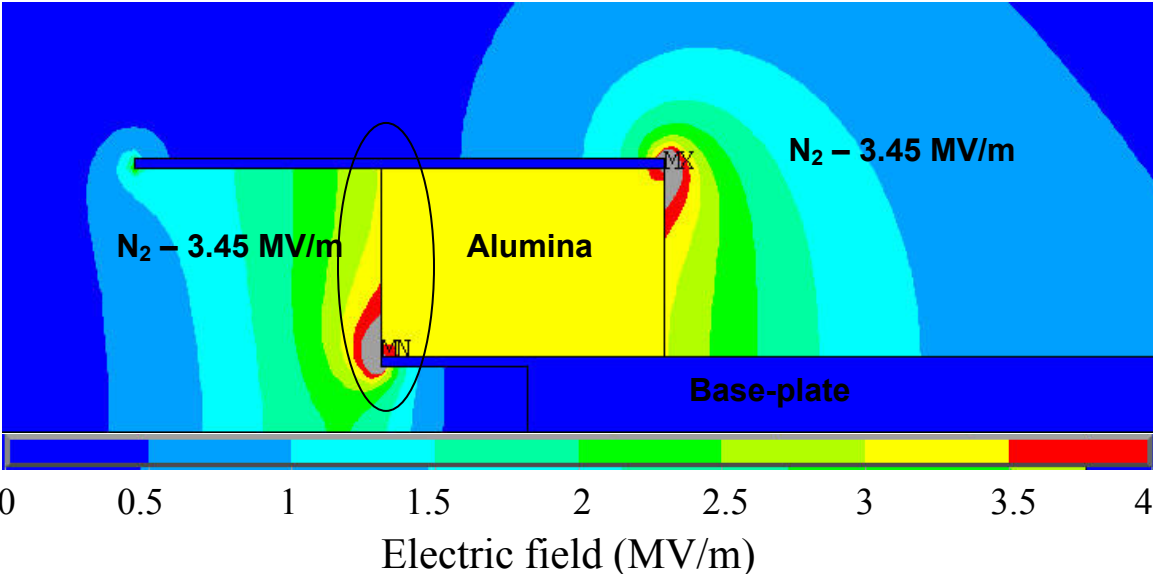


Figure 14. Electric field plot of the Vendor B package under 8-kV operation.

4. Summary

In summary, we have used finite element, electrostatic modeling to design a ceramic package for the next generation of high voltage semiconductor components. This new package is designed to operate at 15 kV, which is more than 5 times higher than conventional ceramic package designs. Our results show that this package will perform successfully without arcing at the lead region and with proper encapsulation and potential termination at the edge of the die, critical electric fields are not exceeded within the die cavity.

Distribution List

Admnstr
Defns Techl Info Ctr
ATTN DTIC-OCP (Electronic copy)
8725 John J Kingman Rd Ste 0944
FT Belvoir VA 22060-6218

DARPA
ATTN IXO S Welby
3701 N Fairfax Dr
Arlington VA 22203-1714

Ofc of the Secy of Defns
ATTN ODDRE (R&AT)
The Pentagon
Washington DC 20301-3080

US Army TRADOC
Battle Lab Integration & Techl Dirctr
ATTN ATCD-B
10 Whistler Lane
FT Monroe VA 23651-5850

Dir for MANPRINT Ofc of the
Deputy Chief of Staff for Prsnl
ATTN J Hiller
The Pentagon Rm 2C733
Washington DC 20301-0300

US Military Acdmy
Mathematical Sci Ctr of Excellence
ATTN LTC T Rugenstein
Thayer Hall Rm 226C
West Point NY 10996-1786

SMC/GPA
2420 Vela Way Ste 1866
El Segundo CA 90245-4659

US Army ARDEC
ATTN AMSTA-AR-TD
Bldg 1
Picatinny Arsenal NJ 07806-5000

US Army Avn & Mis Cmnd
ATTN AMSMI-RD W C McCorkle
Redstone Arsenal AL 35898-5240

US Army Info Sys Engrg Cmnd
ATTN AMSEL-IE-TD F Jenia
FT Huachuca AZ 85613-5300

US Army Natick RDEC
Acting Techl Dir
ATTN SBCN-TP P Brandler
Kansas Street Bldg78
Natick MA 01760-5056

US Army Simulation Train &
Instrmntn Cmnd
ATTN AMSTI-CG M Macedonia
12350 Research Parkway
Orlando FL 32826-3726

US Army Tank-Automtv Cmnd RDEC
ATTN AMSTA-TR J Chapin
Warren MI 48397-5000

Hicks & Assoc Inc
ATTN G Singley III
1710 Goodrich Dr Ste 1300
McLean VA 22102

Palisades Inst for Rsrch Svc Inc
ATTN E Carr
1745 Jefferson Davis Hwy Ste 500
Arlington VA 22202-3402

Director
US Army Rsrch Lab
ATTN AMSRD-ARL-RO-D JCI Chang
PO Box 12211
Research Triangle Park NC 27709

US Army Rsrch Lab
ATTN AMSRD-ARL-D J M Miller
ATTN AMSRD-ARL-CI-IS Mail & Records Mgmt
ATTN AMSRD-ARL-CI-OK-T Techl Pub (2 copies)
ATTN AMSRD-ARL-CI-OK-TL Techl Lib (2 copies)
ATTN AMSRD-ARL-SE-DP D Ibitayo
ATTN AMSRD-ARL-SE-DP W Tipton
Adelphi MD 20783-1197